Experimental and Analytical Studies on Behavior of Curved Composite Box Girders

Experimental and Analytical Studies on Behavior of Curved Composite Box Girders

Yasunori ARIZUMI*, Sumio HAMADA** and Takeshi OSHIRO*

Abstract

The distortional response and slip behavior of curved composite box girders were investigated. Three curved composite box girders with only end diaphragms were tested in order to provide additional informations on the distortional and slip behavior of curved composite box girders. The test specimens were fabricated considering different radii, cross sections and placements of shear connectors. The test results were compared with analytical results based on the curved beam theory and distortional theory proposed by Dabrowski, and on the finite strip method. These results are in good agreement. A parametric study was conducted to discuss the effects of cross-sectional deformations on the stresses of the girder.

Key Words: Box Girder, Composite Structures, Distortion, Tests.

1. INTRODUCTION

Curved box girders, which have high torsional rigidity, are being more widely built. The design analysis of curved box girders must include the stresses due to torsional moment and bimoment as well as bending moment.[1)2)] Further, the effects of cross-sectional deformations must be considered. If a sufficient number of intermediate diaphragms is not provided, high distortional warping stresses are produced, and the effects of cross-sectional deformations cannot be neglected in the design analysis. In Curved composite box girders, the shear force on shear connectors has components in longitudinal and radial directions, and the total force is defined as the resultant. Nevertheless, the available informations on distortional stresses and shear forces on shear connectors of curved composite box girders seem still to be limited.

Theoretical studies of curved box girders dealing with bending moment, torsional moment and bimoment have been conducted, e.g., by Vlasov[3)] and Komatsu.[4)] Analytical studies on

Received: May 9, 1987.

* Department of Architectural Engineering, Faculty of Engineering.

** Department of Civil Engineering, Faculty of Engineering, Yamaguchi University.

cross-sectional deformations of curved box girders have been reported by several researchers. These studies are based on the thin-walled beam theory,[3] folded plate theory,[5] BEF analogy,[6] beam analogy,[7] finite element method,[8] finite strip method[9] and block finite element method.[10] The design procedures on intermediate diaphragms of curved box girders have been studied by Oleinik and Heins,[11] Sakai and Nagai[7] and Nakai and Murayama.[12]

There are several theoretical and experimental studies on curved steel-concrete composite girders having an I-section.[13][14] Very few investigations have been conducted on curved composite box girders. Parametric studies on distortional stresses of curved composite box girders were conducted by Heins[11] and Turkstra.[8] Field test results have also been presented by Heins[15] on a two-span continuous curved composite box girder bridge with a relatively small radius of curvature located in Seoul, Korea.

The present paper aims to study the distortional and slip behavior of simple supported curved composite box girders on the basis of elastic analysis and static tests. The cross-sectional deformations were herein calculated based on the theory proposed by Dabrowski.[6] Test specimens were fabricated, where parameters included different radii, cross sections and placements of shear connectors. Test results are compared with theoretical values based on the curved beam theory and the distortional theory, and with analytical values based on the finite strip method including the spring element of the shear connectors.[16] A parametric study was conducted to evaluate the effects of cross-sectional deformations on the stresses of curved composite box girders.

2. THEORY

The total normal stress σ of curved box girders consists of three components of stresses, i.e., normal bending stress σ_b, torsional warping stress σ_w and distortional warping stress σ_{Dw}, which is given as

$$\sigma = \sigma_b + \sigma_w + \sigma_{Dw} \tag{1}$$

The normal bending stress and torsional warping stress are calculated by the following classic equations ;

$$\sigma_b = \frac{M_x}{I_x} y \tag{2}$$

$$\sigma_w = \frac{B_m}{I_w} \omega \tag{3}$$

where M_x = bending moment, B_m = bimoment, I_x = moment of inertia, I_w = warping constant and ω = warping function.

The differential equation for cross-sectional deformations of a curved box girder shown in Fig. 1 is developed by Dabrowski[6] as follows;

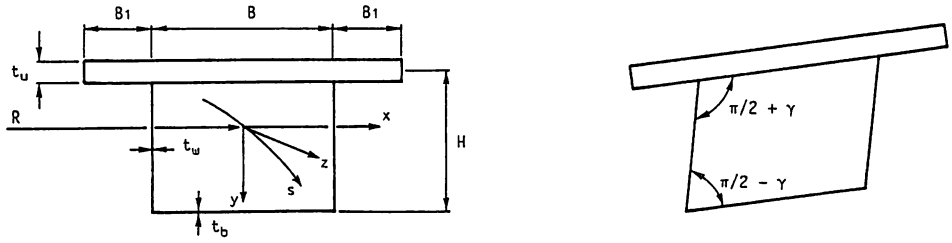

(a) Idealized Cross Section (b) Cross-Sectional Deformation

Fig. 1 Cross Section and Distortion.

$$\left.\begin{aligned} &\frac{d^4\gamma}{ds^4} + 4\lambda^4\gamma = \frac{1}{EI_{Dw}}\left(\rho\frac{M_x}{R} + \frac{m}{2}\right) \\ &\lambda^4 = K_f/4EI_{Dw} \end{aligned}\right\} \tag{4}$$

where γ =angular distortion, E=modulus of elasticity, I_{Dw}=distortional warping constant, ρ=dimensionless shape coefficient, M_x=bending moment, R=radius of curvature, m= distributed external distortional load per unit length and K_f=frame stiffness of a box section per unit length. Eq. (4) indicates that the cross sectional deformations of curved box girders are affected by the magnitude of bending moment. The solution of Eq. (4) can be calculated by using the finite difference method. The high order finite difference form of Eq. (4) at a typical point i is expressed as[18]

$$[-1,\ 12,\ -39,\ 56 + 24\lambda^4\Delta^4,\ -39,\ 12,\ -1] \begin{bmatrix} \gamma_{i-3} \\ \gamma_{i-2} \\ \gamma_{i-1} \\ \gamma_i \\ \gamma_{i+1} \\ \gamma_{i+2} \\ \gamma_{i+3} \end{bmatrix} = \frac{6\Delta^4}{EI_{Dw}}\left(\rho\frac{Mx_i}{R} + \frac{m_i}{2}\right) \tag{5}$$

where Δ=finite difference mesh spacing. When the intermediate diaphragms are provided, this equation must be modified to be applicable to the boundary condition of intermediate diaphragms. When an intermediate diaphragm is provided at a typical point i, Eq. (5) is replaced by following finite difference equation,

$$[-1,\ 12,\ -39,\ 56+24\lambda^4\Delta^4(1+\frac{K_D}{K_f\Delta}),\ -39,\ 12,\ -1]\begin{bmatrix}\gamma_{i-3}\\ \gamma_{i-2}\\ \gamma_{i-1}\\ \gamma_i\\ \gamma_{i+1}\\ \gamma_{i+2}\\ \gamma_{i+3}\end{bmatrix}=\frac{6\Delta^4}{EI_{Dw}}(\rho\frac{Mx_i}{R}+\frac{m_i}{2}) \tag{6}$$

where K_D=stiffness of the intermediate diaphragm. The stiffness of the plate diaphragm is given as

$$K_D=Gt_DBH \tag{7}$$

where G=shear modulus and t_D=thickness of plate diaphragm.[12]

The warping moment M_{Dw} and normal warping stress σ_{Dw} due to cross-sectional deformations are given as

$$M_{Dw}=EI_{Dw}\frac{d^2\gamma}{ds^2} \tag{8}$$

$$\sigma_{Dw}=\frac{M_{Dw}}{I_{Dw}}\omega_{Dw} \tag{9}$$

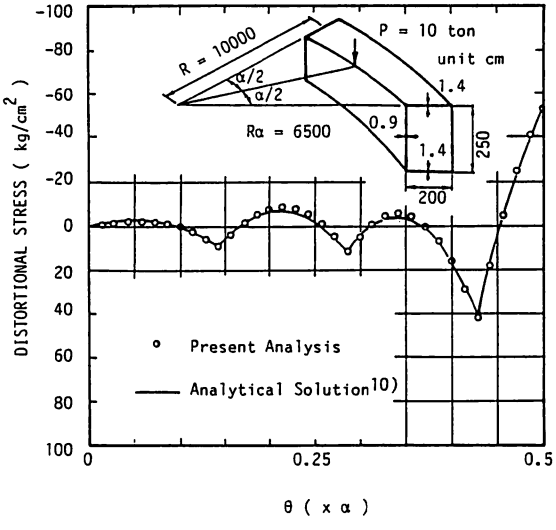

Fig. 2 Distortional Warping Stress Distributions.

where ω_{Dw} =distortional warping function.[12] These distortional warping moments and stresses can be evaluated by using the angular distortions.

A simple supported curved box girder shown in Fig. 2 is herein analyzed. This example was taken from Sakai and Nagai.[10] The box girder has six intermediate plate diaphragms with 20 mm thick and equal spacing. The distortional warping stress distributions in the inner side of the top flange are also shown in Fig. 2. The analytical solutions to the differential equations of cross-sectional deformations are compared with the analytical results obtained from the block finite element method. These results are in good agreement.

3. FINITE STRIP ANALYSIS

The finite strip method was also employed in this study. The steel girder and concrete slab were divided into several curved strip elements and the shear connectors were assumed as two-dimensional spring elements having a linear relationship between force and slip. The details for finite strip analysis of curved composite box girders with incomplete interaction are presented in reference (16).

4. TEST PROGRAM

4.1 Test specimens

Test specimens consist of three composite box girders having different cross sections, different radii and the same span length as shown in Fig. 3. The radii and the central angles are 8 meters and 30 degrees for MODELS C−1 and C−3, 4 meters and 60 degrees for MODEL C−2. The span length of these specimens is 4.187 meters. MODELS C−1 and C−2 have the same cross section but different radii. MODEL C−3 has the same radius as MODEL C−1 but a different steel cross section. Dimensions and specific properties of these specimens

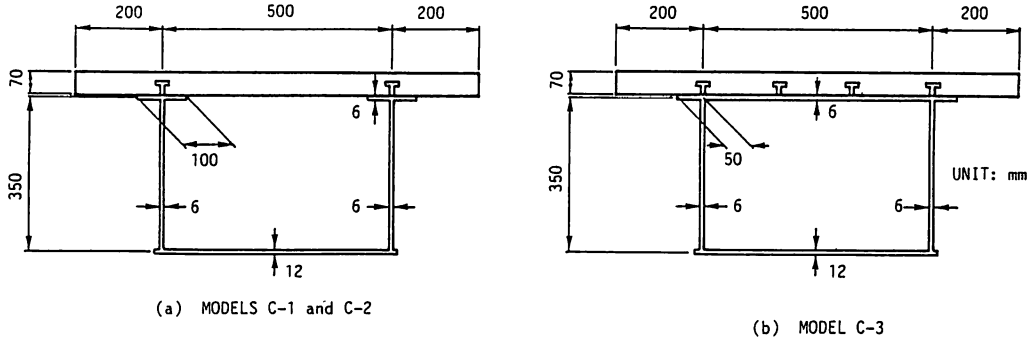

Fig. 3 Tested Curved Composite Girder Sections.

Table 1 Sectional Properties of Test Specimens.

MODEL	RADIUS	CENTRAL ANGLE	STEEL SECTION	AREA OF CROSS SECTION	MOMENT OF INERTIA	ST.VENANT'S TORSIONAL CONSTANT	WARPING CONSTAN	$k=\ell\sqrt{GK/EI_w}$
	R(m)	α(deg.)	(box)	A (cm^2)	I_x (cm^4)	K (cm^4)	I_w (cm^6)	
(1)	(2)	(3)	(4)	(5)	(6)	(7)	(8)	(9)
C−1	8	30	OPEN	206	63045	68132	2526364	43
C−2	4	60	OPEN	206	63045	68132	2526364	43
C−3	8	30	CLOSED	230	66408	71578	2881656	41

are given in Table 1. The values of non-dimensional parameter k for all models are greater than 40.

SS41 steel was used for the steel box girders where the ultimate strength and minimum yield stress are 41 kg/mm² and 24 kg/mm², respectively. The steel flanges were welded to the steel webs. Diaphragm plates with 12 mm thick were attached at the ends of the steel box girders. Intermediate diaphragms were not used; this was for the purpose of surveying cross-sectional deformations. Six deformed reinforcing bars in the longitudinal direction and 23 in the radial direction were placed at the middle surface of a concrete slab with 90 cm wide and 7 cm thick. A cylinder compression test conducted at the time of the testing of the curved composite box girders indicated a strength of 308 kg/cm² and a Young's modulus of 2.85×10^5 kg/cm².

Headed stud shear connectors measuring 13 mm in diameter and 50 mm in height were welded to the top flanges of the steel girders. The number of shear connectors used was 52 for MODELS C−1 and C−2, and 56 for MODEL C−3. The shear connectors of MODELS C−1 and C−2 were provided over each of the webs, with equal spacing. Since MODEL C−3 has the top steel flange plate, the shear connectors were placed in four rows with equal spacing.

4.2 Test equipment and procedure

The test girders were designed as simple supports for bending and fixed supports for torsion in the present experiment. In order to resist negative reactions due to torsional moment of the curved girder, a supporting girder system which was fixed with the movable bearing plate units was employed at the beam ends, as shown in Fig. 4. Two-point loads were applied to the concrete slab on the inner and outer webs at the midspan using a loading beam unit and a hydraulic jack.

4.3 Instrumentations

Measurements of strains in the steel section and concrete slab were conducted by means of electric resistance gages at the section located 30 cm from the midspan(section A−A′) and 30 cm from the end (section B−B′), as shown in Fig. 5. Rosette gages were employed to

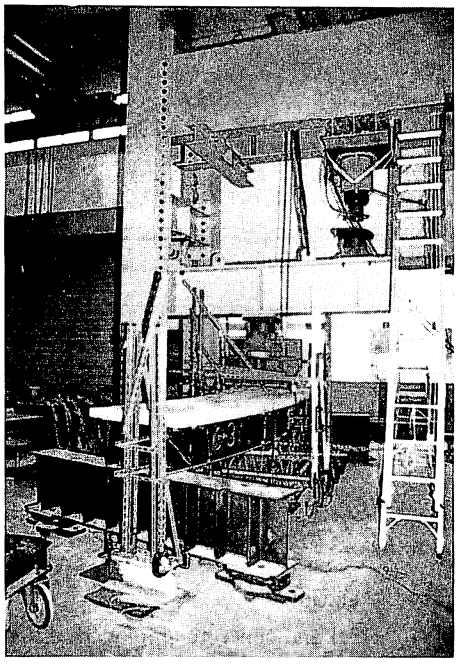

Fig. 4 Setup of a Test Beam.

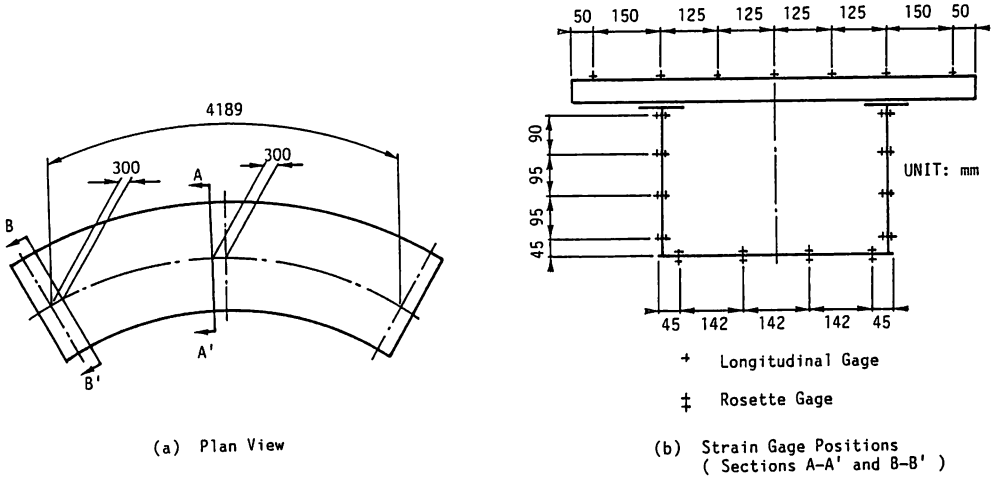

(a) Plan View

(b) Strain Gage Positions (Sections A-A' and B-B')

Fig. 5 Strain Gage Positions.

obtain shear strains in the steel sections.

Deflections and transverse deformations were measured by means of deformation gages at section A−A′, as shown in Fig. 6. Since reaction spreader beams were set up at the ends, deflections and transverse deformations were also measured at the end sections. Measurements

of slips between the concrete slab and steel beam were conducted by means of deformation gages. Locations of slip measurements are shown in Fig. 6.

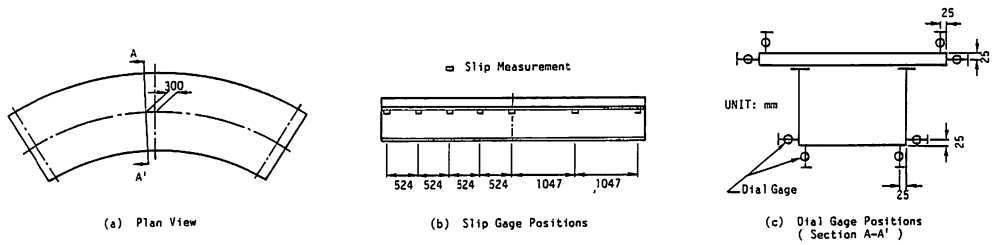

Fig. 6 Locations of Instruments.

5. TEST AND THEORETICAL RESULTS

5.1 Material properties and idealization

The moduli of elasticity for steel and concrete employed in the theoretical analysis were 2.1×10^6 kg/cm² and 3.0×10^5 kg/cm², respectively, based on the material tests. Shear moduli and Poisson's ratios of steel and concrete were 8.1×10^5 kg/cm², 1.29×10^5 kg/cm², 0.3 and 0.167, respectively. In the finite strip analysis, 50 ton/cm was used for the load-slip modulus of a shear connector in both the longitudinal and radial directions. The concrete slab, web and lower flange were divided into 13, 7 and 7 strips, respectively. Thirty-nine terms of the Fourier series were computed; sufficient accuracy was believed to be obtained.

5.2 Cross-sectional deformations

Fig. 7 shows the deformed shapes of section A−A′, which indicates that the deflections on the inner side are greater than those of the outer side. The cross-sectional deformations are affected by the radius of curvature; they become larger as the radius of curvature becomes smaller. MODEL C−3 has greater stiffness and yield smaller cross-sectional deformations compared to MODEL C−1.

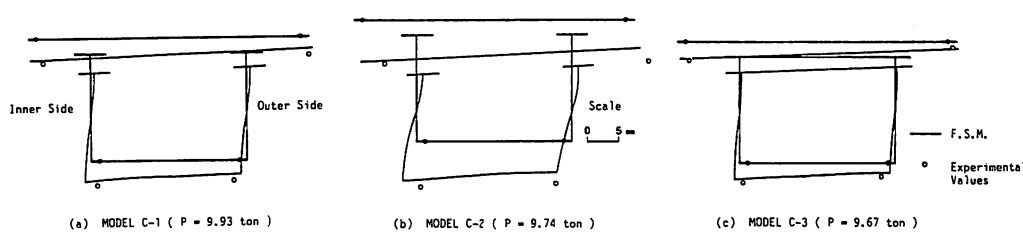

Fig. 7 Deformed Shapes of the Section A−A′.

5.3 Longitudinal stress distributions

The longitudinal stress distributions at section A−A′ are shown in Figs. 8 to 10. In these figures, the longitudinal bending stress and distortional warping stress obtained by the curved beam theory and the distortional analysis are separated from the longitudinal total stress. The longitudinal torsional warping stresses are not shown because they are much smaller than the bending and distortional stresses. These figures indicate that large longitudinal stresses on the inner side occur due to cross-sectional deformations. From the comparison of MODELS C−1 and C−2, the distortional warping stresses seem clearly to be affected by the radius of curvature; the smaller radius provides larger distortional stresses. Longitudinal stress distributions on the outer web seem to be more complex, and may be affected by out-of-plane deformations. Studies conducted by Kuranishi et. al.[18] indicated that in-plane stress distributions of a cylindrical web panel are not linear under a constant bending moment, and that the compressive part near the upper fiber has large stresses. The present test and analytical results also demonstrate similar performances. This tendency is prominent on the inner web of MODEL C−2.

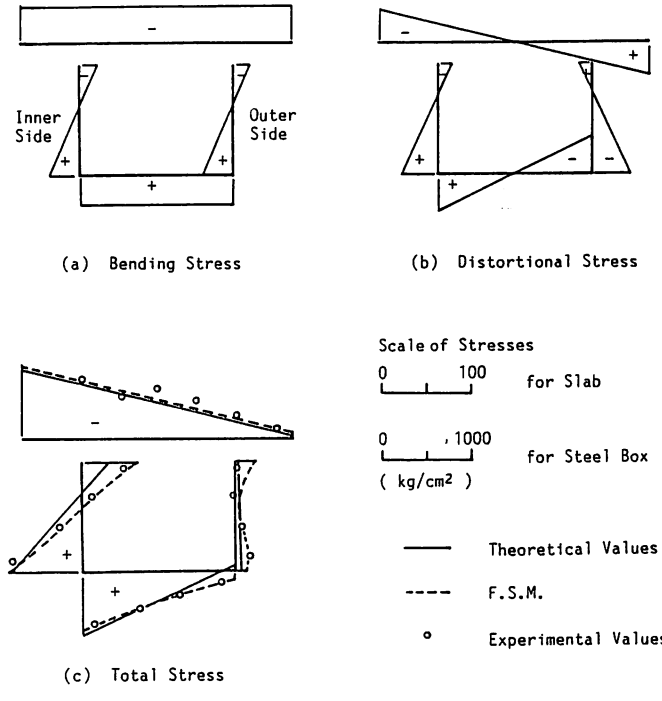

Fig. 8 Longitudinal Stress Distributions at the Section A−A′ of MODEL C−1 (P=9.93 ton).

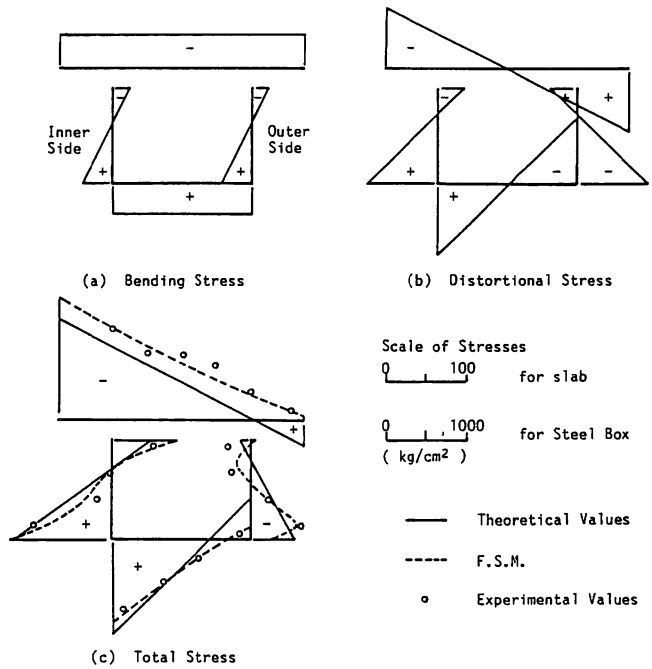

Fig. 9 Longitudinal Stress Distributions at the Section A−A′ of MODEL C−2 (P=9.74 ton).

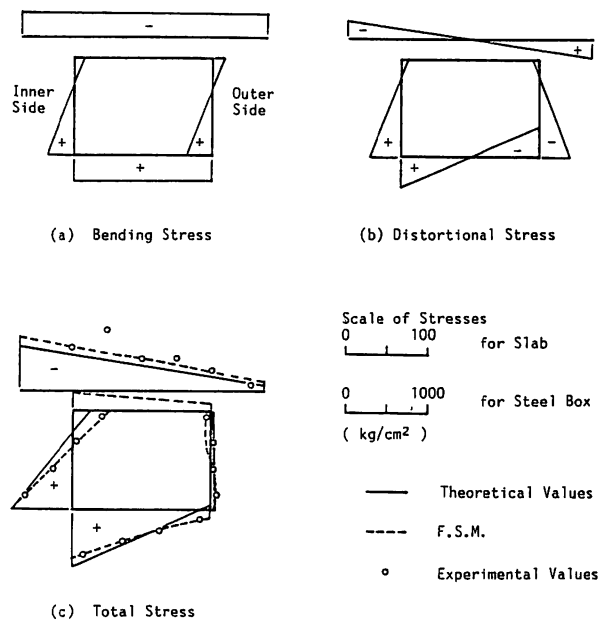

Fig. 10 Longitudinal Stress Distributions at the Section A−A′ of MODEL C−3 (P=9.67 ton).

5.4 Shear stress distributions

Shear stress distributions at section B−B′ are shown in Figs. 11 to 13. The shear stresses in the outer web are fairly large compared to the ones in the inner web. This requires careful consideration in the design of the outer web for shear and torsion. However, the shear stresses in the concrete slab of MODEL C−3 are relatively smaller than those of MODEL C−1. This implies that the torsion to which the composite box section subjected is mostly resisted by the steel box section.

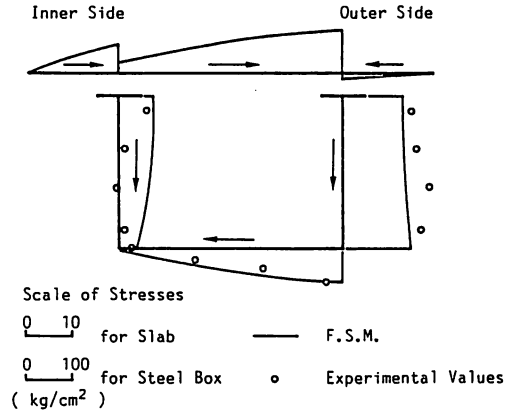

Fig. 11 Shear Stress Distributions at the Section B−B′ of MODEL C−1 (P= 9.93 ton).

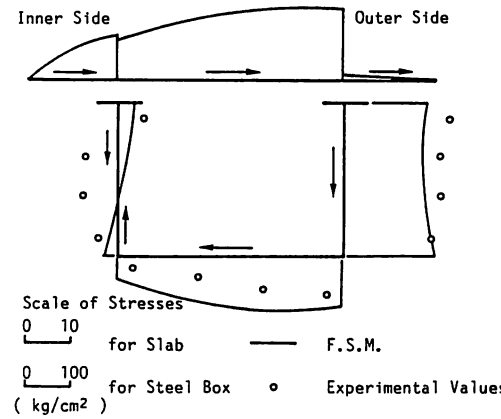

Fig. 12 Shear Stress Distributions at the Section B−B′ of MODEL C−2 (P= 9.74 ton).

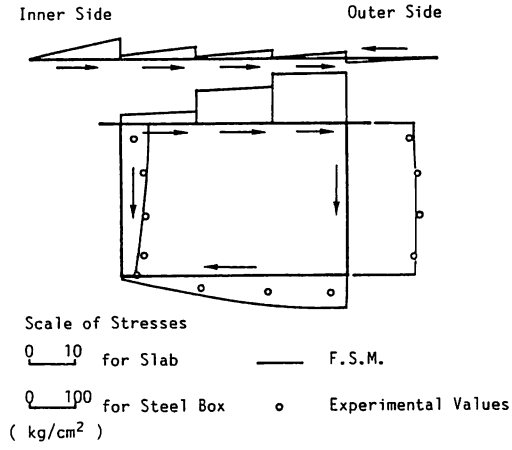

Fig. 13 · Shear Stress Distributions at the Section B−B′ of MODEL C−3 (P=9.67 ton).

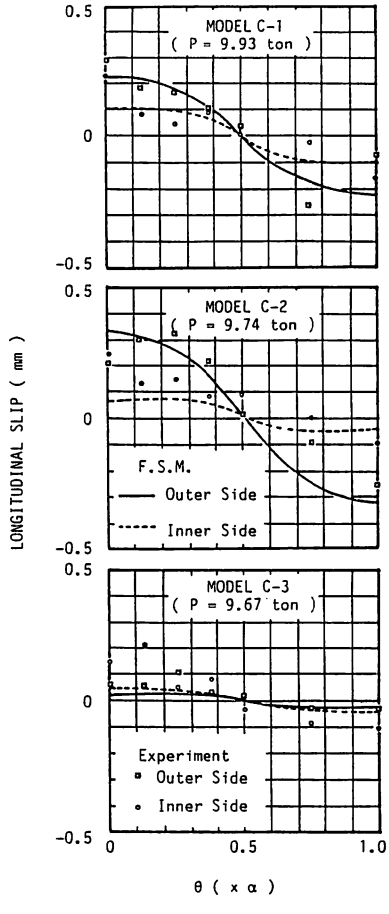

Fig. 14 Longitudinal Slip Distributions.

5.5 Longitudinal slip distributions

Longitudinal slip distributions between the concrete slab and the steel girder are shown in Fig. 14. This figure indicates that the slip on the outer web of MODEL C−1 are relatively greater than those on the inner web. This tendency also occurs in MODEL C−2. The slips are affected by torsion as well as by shear force, and become larger as the radius of curvature diminishes. On the other hand, the slips of MODEL C−3 are smaller than those of MODEL C−1.

5.6 Radial slip distributions

Radial slip distributions are shown in Fig. 15. Radial slip obtained by the finite strip analysis are extremely small compared to the experimental ones, since no radial displacement of the concrete slab is assumed at the end. This figure indicates that fairly large slips occurred at the ends of the girder having an open steel section, and that MODEL C−2 gives larger slips. This may have resulted from the influence of curvature. The values of slips of MODEL C−3, however, are relatively small, probably due to the placement of shear connectors on the upper flange.

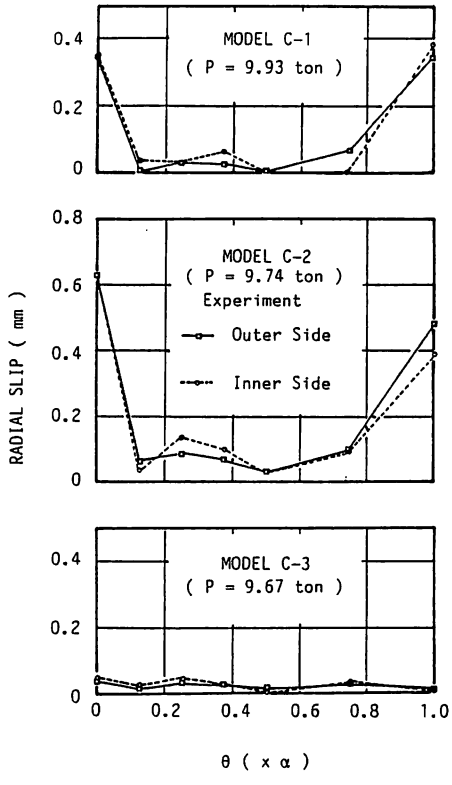

Fig. 15 Radial Slip Distributions.

6. PARAMENTRIC STUDY

The present analytical results of normal stresses based on the curved beam theory and the distortional theory proposed by Dabrowski are in good agreement with experimental results for all test girders. A part of this study aims to discuss the simplified design equations for distortional stresses proposed by Oleinik and Heins[11], Nakai and Murayama[12] and Sakai and Nagai.[7] The distortional effects are herein discussed for curved composite box girders with a single cell subjected to a uniformly distributed load and an eccentric concentrated load. The normal stresses due to cross-sectional deformations are obtained by using the finite difference method. Variable parameters are intermediate diaphragm spacing, the central angle and width of the extended concrete slab. Details of the cross sections of curved composite box girders herein analyzed are shown in Fig. 16. The span lengths for MODELS C−L and C−H are 50

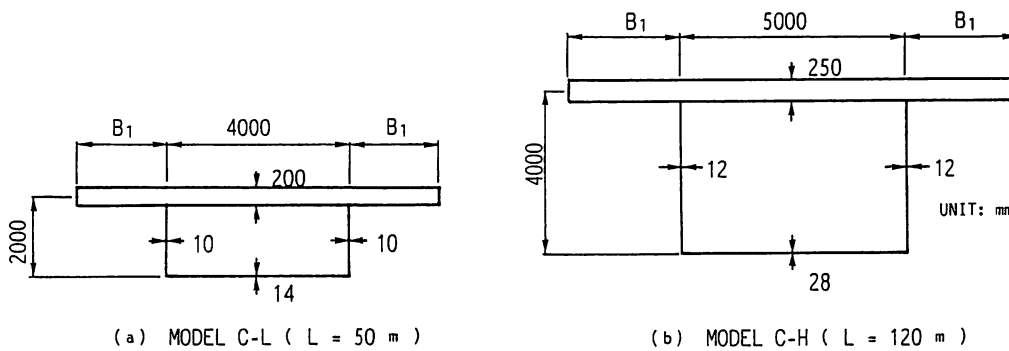

Fig. 16 Composite Sections for Parametric Study.

meters and 120 meters, respectively. Intermediate diaphragms with infinite stiffness are assumed in all cases. Two loadings, which consisted of a uniformly distributed and an eccentric concentrated loads, are used in the study. An eccentric concentrated load is positioned over the interior web at the center cross section between one diaphragm at (or near) the midspan and the adjacent one. The results of the parametric study are shown as the ratio of maximum distortional warping stress in the bottom flange to the maximum bending stress. The maximum distortional warping stresses are produced at the cross section with an intermediate diaphragm at (or near) the midspan when a uniformly distributed load is applied and produced at the loaded cross section when an eccentric concentrated load is applied. The present analytical results are compared with the results based on the simplified design equations proposed by other researchers. Simplified design values proposed by Oleinik and Heins under a concentrated load are not herein shown, because different loading conditions are used.

6.1 Effects of intermediate diaphragm spacing

Effects of the intermediate diaphragm spacing are shown in Figs. 17 and 18 for curved

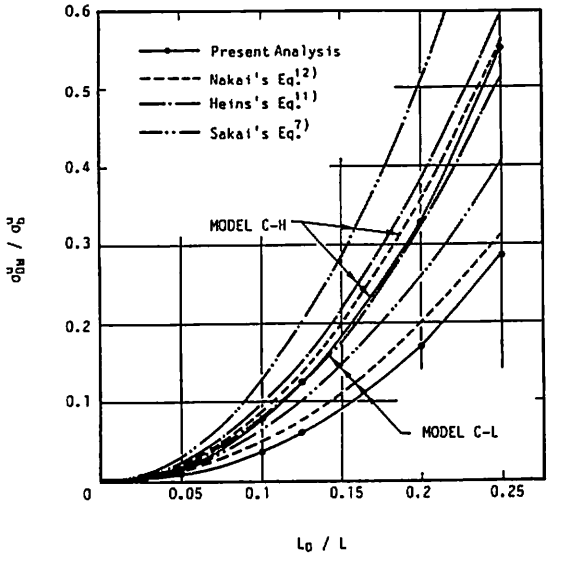

Fig. 17 Stress Ratios with Respect to Diaphragm Spacing under Uniformly Distributed Load.

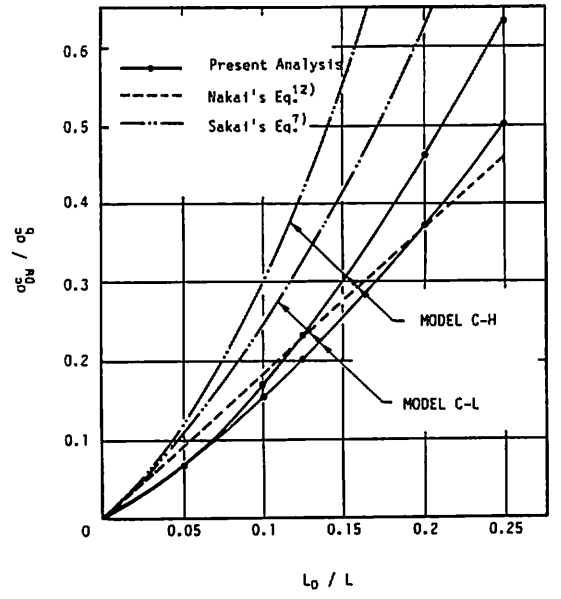

Fig. 18 Stress Ratios with Respect to Diaphragm Spacing under Concentrated Load.

girders with a central angle of 60 degrees and an extended concrete slab width ratio of 0.5 to web spacing, B_1/B. These figures show relationships between the stress ratio and the diaphragm spacing ratio to span, L_D/L. The stress ratios increase in proportion to the diaphragm spacing ratio. A comparison of Figs. 17 and 18 indicates that eccentric concentrated loads produce higher distortional stresses than a uniformly distributed load. In the case of $(\sigma_{Dw}/\sigma_b)<10\%$, the simplified design values are larger than the present results. If a sufficient number of diaphragms are provided, the effects of cross-sectional deformations may be disregarded in the design analysis of curved composite box girders.

6.2 Effects of curvature

The stress ratios with respect to the central angle are shown in Figs. 19 and 20. The

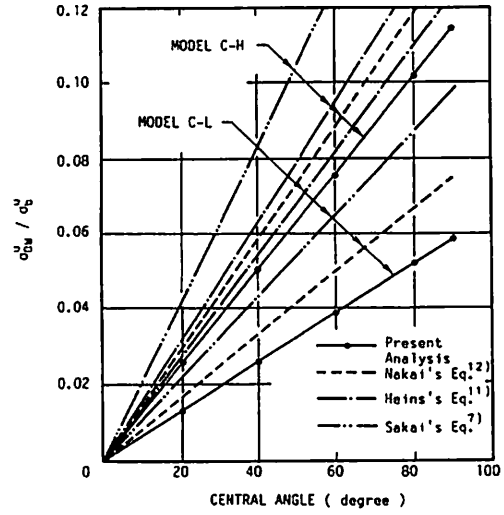

Fig. 19 Stress Ratios with Respect to Central Angle under Uniformly Distributed Load.

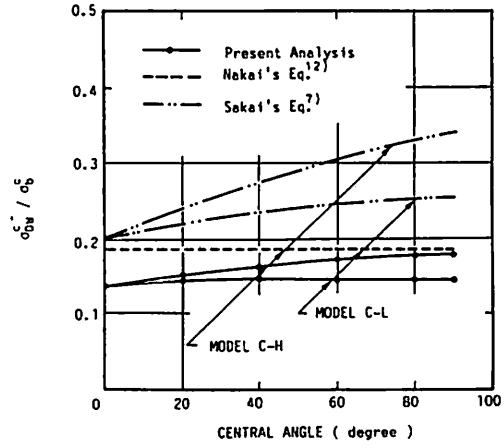

Fig. 20 Stress Ratios with Respect to Central Angle under Concentrated Load.

curved girders herein analyzed have a diaphragm spacing ratio of 0.1 and an extended slab width ratio of 0.5. The stress ratios under a uniformly distributed load increase in proportion to the central angle, whereas under an eccentric concentrated load they do not show much increase.

6.3 Effects of extended slab width

The results for curved girders with a central angle of 60 degrees and a diaphragm spacing ratio of 0.1 are shown in Figs. 21 and 22. The extended slab width ratios vary from 0 to

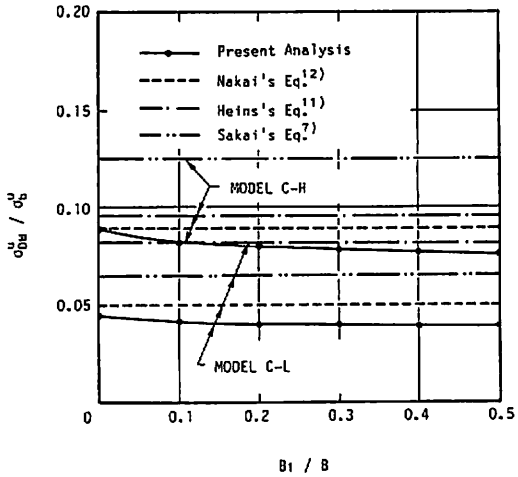

Fig. 21 Stress Ratios with Respect to Extended Slab Width under Uniformly Distributed Load.

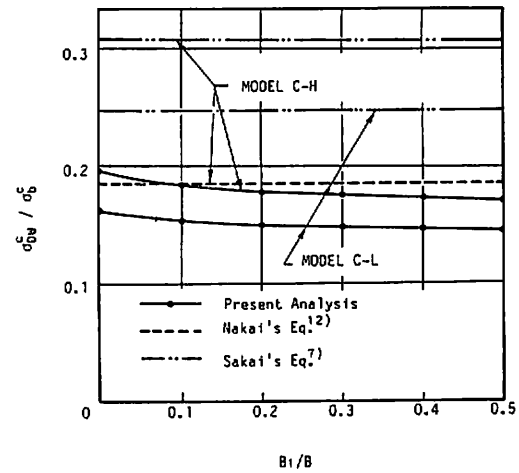

Fig. 22 Stress Ratios with Respect to Extended Slab Width under Concentrated Load.

0.5 . The stress ratio decreases slightly with increase in the extended slab width. For curved girders, however, the extended slab width does not have any significant effect.

7. CONCLUSIONS

The distortional and slip behavior of simple supported curved composite box girders were investigated analytically and experimentally. Analyses were based on the courved beam theory and the distortional theory proposed by Dabrowski, and on the finite strip method including effect of slips between the concrete slab and steel girder. Three courved composite girders were tested in order to provide additional informations on cross-sectional deformations and its effect on stresses and slips between the concrete slab and steel girder. Parametric studies were conducted to evaluate stresses due to cross-sectional deformations in which diaphragm spacing, curvature and extended slab width were varied. The major conclusions from the present investigation are:

1. The cross-sectional deformations of curved composite box girders with only end diaphragms are considerably large, and produce large additional longitudinal stresses.

2. Longitudinal stress distributions in the web section are complex, which may be due to the out-of-plane deformation. This behavior is particularly remarkable in the girders having a small radius of curvature.

3. Longitudinal forces acting on the studs are affected by torsion as well as by shear force. Special attention must be paid to the radial forces acting on the studs in the end region of the girders having an open steel section.

4. Compared to open steel sections, closed steel sections with the studs placed on the top flange provide a good effect on longitudinal and radial forces which act on the studs.

5. The longitudinal stresses due to cross-sectional deformations increase with the diaphragm spacing and the central angle.

6. An increase in the extended concrete slab width decreases slightly the distortional stress ratio.

ACKNOWLEDGMENTS

This research was sponsored by the Science Research Subsidy of the Japanese Ministry of Education (No. 59750359, No. 60750433). All steel girders used in the present test were fabricated by Okazaki Kogyo Co. Ltd. S. Kawazoe and R. Shokyu of Okazaki Kogyo Co. Ltd. collaborated on the initial planning and fabrication of the specimens. The authors gratefully acknowledge with their cooperations and supports.

APPENDIX

The simplified design equations for the stress ratios of distortional warping stress to

bending stress developed by Oleinik and Heins[11], Nakai and Murayama[12] and Sakai and Nagai[7] are the following equations;

(a) for uniformly distributed load

(1) Oleinik and Heins's equation

$$\sigma^u_{Dw} / \sigma^u_b = (10L - 350)s^2/R \tag{10}$$

in which s=diaphragm spacing as a fraction of span length, L=span length (ft.) and R=radius of curvature (ft.).

(2) Nakai and Murayama's equation

$$\sigma^u_{Dw} / \sigma^u_b = (0.8 + 0.32L/B)\alpha\,(L_D/L)^2 \tag{11}$$

in which L_D=diaphragm spacing, L=span length, α=central angle and B=web spacing.

(3) Sakai and Nagai's equation

$$\sigma^u_{Dw} / \sigma^u_b = (L/B)\alpha(L_D/L)^2/2 \tag{12}$$

(b) for a concentrated load

(1) Oleinik and Heins's equation

$$\sigma^c_{Dw} / \sigma^c_b = (-0.25 \times 10^{-2}\, L + 1.3)s \tag{13}$$

(2) Nakai and Murayama's equation

$$\sigma^c_{Dw} / \sigma^c_b = -1.85(L_D/L) \tag{14}$$

(3) Sakai and Nagai's equation

$$\sigma^c_{Dw} / \sigma^c_b = 2(L_D/L)/r_c + (L/B)\,(L_D/L)^2\alpha/2 \tag{15}$$

in which $r_c = 2(R/L)\tan(\alpha/2)$.

REFERENCES

1. The task subcommittee on box girders of the ASCE−AASHTO committee on flexural members of the committee on metals of the ASCE structural division: Curved steel box girder bridges: State-of-the-art, Journal of the Structural Division, ASCE, Vol. 104, No. ST 11, pp. 1719−1739, 1978.
2. The subcommittee on ultimate strength of box girders of the ASCE−AASHTO task

committee on flexural members of the committee on metals of the structural division : Steel box-girder bridge—Ultimate strength considerations, Journal of the Structural Division, ASCE, Vol. 100, No. ST 12, pp. 2433—2448, 1974.

3. Vlasov, V.Z. : Thin-walled elastic beams, National Science Foundation, 1961.
4. Konishi, I. and Komatsu, S. : Three dimensional analysis of simply supported curved girder bridges (in Japanese), Transactions of the Japan Society of Civil Engineers, No. 90, pp. 11—26, 1963.
5. Alam, K.M., Honglandaromp, T. and Lee, S.L. : Curved box girder bridges with intermediate diaphragms and supports, Pub. of IABSE, Vol. 33—II, 1973.
6. Dabrowski, R. : Curved thin-walled girders, Theory and analysis, Springer-Verlag, Berlin, Germany, 1968.
7. Sakai, F. and Nagai, M. : A proposal for intermediate diaphragm design in curved steel box girder bridges (in Japanese), Procceedings of the Japan Society of Civil Engineers, No. 305, pp. 11—22, 1981.
8. Turkstra, C.J. and Fam, R.M. : Behavior study of curved box bridges, Journal of the Structural Division, ASCE, Vol. 104, No. ST 3. pp.453—462, 1978.
9. Cheung, Y.K. : Finite strip method in structural analysis, Pergamon Press, 1976.
10. Sakai, F. and Nagai, M. : Three-dimensional analysis of thin-walled curved box girders by block finite element method (in Japanese), Proceedings of the Japan Society of Civil Engineers, No. 295, pp.1—13, 1980.
11. Oleinik, J.C. and Heins, C.P. : Diaphragms for curved box beam bridges, Journal of the Structural Division, ASCE, Vol. 101, No. ST10, pp.2161—2178, 1975.
12. Nakai, H. and Murayama, Y. : Distortional stress analysis and design aid for horizontally curved box girder bridges with diaphragms (in Japanese), Proceedings of the Japan Society of Civil Engineers, No. 309, pp. 25—39, 1981.
13. Colville, J. : Test of curved steel concrete composite beams, Journal of the Structural Division, ASCE, Vol. 99, No. ST 7, pp.1555—1570, 1973.
14. Maeda, Y., et al. : Static test of two-span continuous curved composite girders (in Japanese), Dept. of Civil Engrg., Osaka Univ., 1973.
15. Heins, C.P. and Lee, W.H. : Curved box-girder bridges : Field test, Journal of the Structural Division, ASCE, Vol.107, No.ST 2, pp.317—327, 1981.
16. Arizumi, Y., Oshiro, T. and Hamada, S. : Finite strip analysis of curved composite girders with incomplete interaction, Computers & Structures, Vol. 15, No.6, pp.603—612, 1982.
17. Collatz, L. : The numerical treatment of differential equations, Springer, 1960.
18. Kuranishi, S. and Hiwatashi, S. : Elastic behavior of web plates of curved plate girders in bending (in Japanese), Proceedings of the Japan Society of Civil Engineers, No. 315, pp.1—11, 1981.

NOTATION

The following symbols are used in this paper :

A = area of cross section
B = web spacing
B_1 = extended concrete slab width
B_m = bimoment
E = modulus of elasticity
G = shear modulus
I_{Dw} = distortional warping constant
I_w = warping constant
I_x = moment of inertia
K = St. Venant's torsional constant
K_D = stiffness of intermediate diaphragm
K_f = frame stiffness of a unit length of a box section
k = $L\sqrt{GK/EI_w}$
L = span length
L_D = intermediate diaphragm spacing
M_x = bending moment
m = distributed external distortional load per unit length
R = radius of curvature
t_D = thickness of diaphragm plate
α = central angle
γ = angular distortion
Δ = finite difference mesh spacing
ρ = dimensionless shape coefficient
σ = total normal stress
σ_b = normal bending stress
σ_{DW} = normal distortional warping stress
σ_w = normal torsional warping stress
ω = warping function and
ω_{DW} = distortional warping function.